NUMERICAL INVESTIGATION OF WATER FLOWS INSIDE A MICROCHANNEL

AHMAD KAMIL BIN MOHD TARMIJI

This report is submitted

in fulfillment of the requirement for

Bachelor of Mechanical Engineering

Faculty of Mechanical Engineering

UNIVERSITI TEKNIKAL MALAYSIA MELAKA

2018

DECLARATION

I declare that this project entitled "Numerical Investigation of Water Flows Inside a Microchannel" is the result of my own work except as cited in the reference.

Signature: ………………………………….

Name: AHMAD KAMIL BIN MOHD TARMIJI

Date:…………………...2018

APPROVAL

I hereby declare that I have read this project, and, in my opinion, this report is sufficient in terms of scope and quality for the award of the Bachelor of Mechanical Engineering (with Honours).

Signature: ……………………………

Name: DR ERNIE BT MAT TOKIT

Date :……………………2018

DEDICATION

To my beloved father and mother MOHD TARMIJI BIN MUKHTAR and MARIAH BINTI SELAMAT .

My supervisor DR ERNIE BT MAT TOKIT

And dear friends.

ABSTRACT

In this study, by using water as a cooling fluid, the three-dimensional fluid flow and heat transfer in a rectangular micro-channel are analyzed numerically. The microchannel have a depth of 180 μm and a width of 57 μm, and length of 10 mm. A numerical analysis is simulated using a Gambit 2.4.6 and Fluent 6.1 version. The results carefully validated by comparing the data with the other available experiment data. In terms of velocity profiles, flow Reynolds number affects the length of the flow developing region. For the higher value of Reynold number of 1500, fully developing region may not be achieved. It is also found that the temperature rises along the flow directional in the solid and fluid region can be approximately linear for the microchannel investigation. Temperature is high at the channel top wall rather than channel bottom wall with the deviation of 0.51%. At near channel inlet, the Nusselt number much more higher values and vary around the channel periphery, approaching 5 average Nusselt number.

ABSTRAK

Dalam kajian ini, dengan menggunakan air sebagai cecair penyejukan, aliran cecair tiga dimensi dan pemindahan haba dalam Mikrochannel segi empat tepat dianalisis secara berangka. Mikrochannel mempunyai kedalaman 180 µm dan lebar 57 µm, dan panjang 10 mm. Analisis numerik disimulasikan menggunakan Gambit 2.4.6 dan versi Fluent 6.1. Hasilnya disahkan dengan membandingkan data dengan data eksperimen lain yang tersedia. Dari segi profil halaju, aliran bilangan Reynolds mempengaruhi panjang aliran wilayah yang sedang berkembang. Bagi nilai Reynold yang lebih tinggi daripada 1500, rantau membangun sepenuhnya tidak dapat dicapai. Ia juga mendapati bahawa suhu meningkat sepanjang arah aliran di kawasan pepejal dan bendalir boleh menjadi kira-kira linear untuk penyiasatan mikrochannel. Suhu tinggi di dinding atas saluran berbanding dinding bawah saluran dengan perbezaan 0.5%. Di dalam saluran masuk berhampiran, nombor Nusselt mempunyai nilai yang lebih tinggi dan berbeza di sekitar pinggir saluran menghampiri 5 purata nombor Nusselt.

ACKNOWLEDGEMENTS

Praise is to Allah SWT the Almighty and the All Merciful who has given me His blessing, kindness and guidance in leading me to accomplish the final year project. Shalawat and Salam are always delivered to Prophet Muhammad SAW, who has guided his followers to the right patch. Every project whether big or small is successful due to the effort of the number of nice people who always giving advice and helping hand.

I would like to express my deepest gratitude and appreciation to my supervisor Dr. Ernie Binti Mat Tokit from Universiti Teknikal Malaysia Melaka (UTEM) for her invested unwavering support, collegiality, and mentorship throughout this project.

I also would like to thank to second examiner, En. Shamsul Bahari Bin Azraai for his valuable time giving me some advice and tips to accomplish my project. Some special thanks also to my friend, who always guide me through this research.

Lastly, I would like to extend my thanks to both of my parents, Mohd Tarmiji Bin Mukhtar and Mariah Binti Selamat for raising me well and always support me in every situation especially in term of finance. They are my source of strength to complete my project.

TABLE OF CONTENTS

LIST OF FIGURES

FIGURE **TITLE** **PAGE**

LIST OF TABLES

TABLE TITLE PAGE

CHAPTER 1

INTRODUCTION

1.1 Background

Geometry, surface roughness, flow velocity, surface temperature, and type of fluid affect the transition from laminar to turbulent flow inside a microchannel. According to Osborne Reynolds (Cengel & Cimbala, 2014) in 1880 by injecting some dye streaks into the flow in a glass pipe, the author discovered that the flow regime depends on the ratio of internal forces to viscous forces in the fluid that is now called Reynold number. Critical Reynolds number, Re_{cr} is the Reynolds number at which the flow becomes turbulent. For internal flow inside the circular pipe, the Re_{cr} is on 2300. Reynolds number is based on the hydraulic diameter D_h of the pipes. Under the most practical conditions by considering all degree of disturbance of flow by surface roughness, pipe vibrations and fluctuations in the upstream flow, the critical Reynolds number was under transitional flow from 2300 to 4000 Reynolds number.

Small channel measurement studies separated the ranges from 1 µm to 100 µm as a microchannel, 100 µm to 1 mm as meso-channels, 1 mm to 6 mm as reduced entries, and more than 6 mm as compact passages. This group is essentially based on the size of the channel build (Mehendale, Jacob, & Shah, 2000). Classification of flow based on Knudsen number is used for providing a classification scheme for microchannel, small channels, and conventional channels. For this purpose, means normal gas free pathways such as oxygen, nitrogen, and hydrogen near

1 atmospheric pressure is considered. (Satish G. Kandlikar, 2003) classifies its conventionnel channel with more than 3mm its hydraulic diameter. Otherwise, mini-channels from range 3mm to 200µm and microchannel from 200 µm to 10µm. They are prescribed for both liquid and in addition two-phase flow applications to give a consistency in channel characterization.

The velocity profile shows in Figure 1.1 to know the nature of the fluid flow inside a channel. By considering fluid enters circular pipe at a uniform velocity, in no-slip condition, the fluid particle in the layer is completely stopped in contact with the wall of the pipe. In boundary layer region, viscous effects and velocity changes are significant. Otherwise, in irrotational flow region, the frictional effect is negligible, and the velocity remains essentially constant in radial direction. When the velocity profile is fully developed and remain unchanged, it's called hydrodynamically fully developed region. When the fully developed average velocity profile is flatter or fuller, it's totally in turbulence flow. Otherwise, when parabolic, it's a laminar flow (Cengel & Cimbala, 2014).

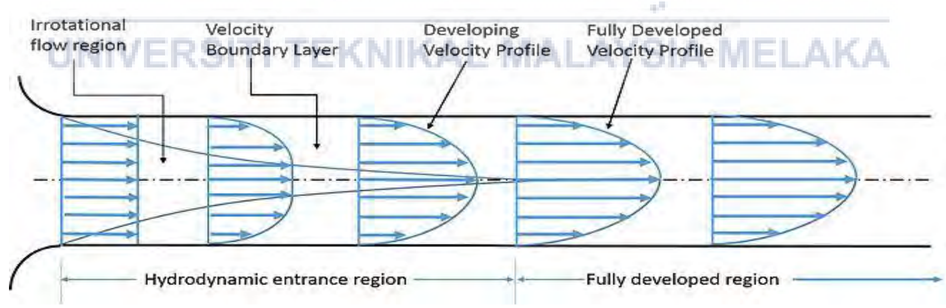

Figure 1.1: The development of the velocity boundary layer in pipe (Cengel & Cimbala, 2014).

Therefore, the aim for this study is to numerically investigate the water flow inside a microchannel. The solid substrate used is copper and water as coolant fluid. The distribution of average temperature and average Nusselt number inside a microchannel been analyze.

1.2 Problem Statement

Theoretically, the critical Reynolds number for internal flows in the circular pipe is 2300. But in some cases, the critical Reynold number can be low as 1700 to 2400. This indicates that the laminar flow region is below the Reynolds number of 1700. The velocity profile for laminar region in the fully developed region is parabolic while turbulence much more flatter and fuller. Therefore, there is a need to verify in the fully developing region either the parabolic velocity profile in the laminar flow is applicable for water flow inside a microchannel.

1.3 Objective

The main objectives of this project are:

1. To simulate the water flow at various Reynolds number in laminar flow.
2. To investigate the velocity profile of water flow at various Reynolds number

1.4 Scope

The performance of the microchannel is analyzed using Computational Fluid Dynamic (CFD) FLUENT 6.1 software. The scopes of this project are:

1. For the microchannel, the hydraulic diameter range of 10 μm – 200 μm and from 1000 to 1500 for the Reynolds number.
2. This research is simulated using a software known as Gambit and Fluent. Only velocity profile of water flow is examined.
3. Only water as working fluid used in the study.

1.5 General Methodology

The actions that need to be carried out to achieve the objectives in this project are listed below.

1. Literature review:

   Books, journals, article and all another alternative reference for this project.
2. Design Drawing:

   The sizing of microchannel using Gambit geometry and mesh generation software.
3. Simulation:

   Simulation of the water velocity profiles using Fluent software based on the various of Reynolds number.
4. Analysis

   The velocity profiles pattern result is analyzed to get the value of the critical Reynolds number.
5. Report writing:

A report on this study is written at the end of the project.

CHAPTER 2

LITERATURE REVIEW

2.1 Introduction

A literature review is a search and evaluation of the available paper or research to the chosen subject. This include the survey of the chosen area of study, synthesizes the information in that literature into a summary, critically analyze information gathered by identifying gaps in current knowledge by showing the limitation and point of views and the formula used in controversial area, where the literature is expressed in an organized way. For this section, all information on the latest research about a way to gathering the critical Reynolds number, laminar, transition and turbulence fluid flow, a factor that influence the critical Reynolds number, and summary of the past literature of study. Other than that, it shows the method used to get the critical Reynolds number in the study.

2.2 Critical Reynolds Number

Investigation of fully developed of liquid and vapor flow through the rectangular microchannel had been done by (Hrnjak & Tu, 2007). The hydraulic diameter used varies from 69.5 to 304.7 µm with the aspect ratio changing from 0.09 to 0.24. Testing fluid, R-134a liquid, and water vapor were used, and the Reynold number varied between 112 to 9180. Experiment was conducted with the surface roughness of 0.21 to 0.48. For the laminar region, turbulent region and transition region, the friction factor was characterized by using pressure drop data. The author claim that even in the smallest channel test, both laminar friction factor and critical Reynold number approximate the conventional value when the surface roughness was low. As a result, the critical Reynold number range is2150 – 2290 for the smooth surface. They also determine that critical Reynold number and laminar friction factor are both significant toward the conventional value when the surface roughness becomes low. As a suggestion, the authors propose that surface roughness were responsible toward the transition to turbulent become early.

An experiment of pressure drop measurement in a microchannel was conducted to a greater understanding of flow in the small channel. The result produced were different compared to the theoretical in a future study of the friction factor for testing fluid of water and transition Reynolds number in rectangular microchannel. The Reynolds number in between 60 – 3450 in a high aspect ratio channel, a hydraulic diameter range of 252 to 973 with depth ranging from 128 to 521 µm and fixed width of 1-cm. The microchannel surface roughness was classified as smooth and a mean surface roughness 1.9 µm of polycarbonate/polyimide, maximum peak value height approximates 14.67 µm and relative roughness of 0.74%. Excluding entrance and exit losses, the pressure drop was measured within the channel itself and the transition from laminar to turbulence was observed with flow image. As a result, the transition value becomes lower than the conventional critical Reynolds number that in range of 1700 to 2200 (Pfund, Rector, Shekarriz, Popescu, & Welty, 2000).

Another experiment was conducted to measure the friction factor of laminar flow of deionized water in smooth silicon microchannel of the trapezoidal cross-section with a range of the hydraulic diameter 25.9 to 291.0 µm. Thirteen different trapezoidal silicon microchannel were observed. It was shows, the cross-sectional aspect ratio effects the friction constant of this microchannel. They also prove that Navier-stokes equation that follows non-slip condition was still applicable for deionized water flow in smooth silicon microchannel in 25.9 µm hydraulic diameter. For smooth channel but high hydraulic diameter of 103.4 to 291.0 µm, the Reynolds number of 1500 to 2000 was found as the transition from laminar to turbulent (Wu & Cheng, 2003).

An investigation of an experiment of the heat transfer and pressure drop in a rectangular microchannel was performed for water in the laminar and transitional regimes for 3 different inlet configurations. Inlet type consists of 0.57 mm, 0.0.85 mm and 1.05 mm hydraulic diameter under consideration of sudden contraction, bellmouth and swirls inlet type. From the experiment, it was found that critical Reynold number and the transition behavior influences by the inlet type. As a result, the critical Reynolds number was in the range of 1800 to 2000 for the unexpected contraction inlet type and the adiabatic friction factors. For diabatic cases, the transition regime starts at 2000 Reynolds number. Both adiabatic and diabatic consist of 2.3 µm surface roughness and 0.0022% of relative roughness. For bellmouth inlet type, the adiabatic transition started at 1250 Reynolds number while diabatic start at 1200. Bellmouth inlet is much smoother than contraction inlet type. Lastly, for swirl inlet type, a major transition occurs on 1600 Reynolds number while minor adjustment occurs at Reynold number 800 (Dirker, Meyer, & Garach, 2014).

Surface roughness within the microchannel seems to have a significant effect on flow behavior at the microscale. Flow transition from laminar flow to turbulent flow at the microscopic level must be studied in greater details so that one may accurately predict at which value of Reynolds number this transition occurs for all wall roughness's.(Hassan, Phutthavong, & Abdelgawad, 2004)

An experimental and numerical analysis of a single-phase flow through the rectangular microchannel of water in the range of the Reynolds number in between 300-3500. Hydraulic diameter considers between 318 µm to 903 µm. The microchannel width ranged from 194 µm to 534 µm, with the depth, was five times in each case. Copper was used as test piece with contained 10 microchannels in parallel. The fluid test used was deionized water. Based on the result, the transition occurs at Reynold number of 1500 to 2000. At this moment, the result showed slope, reflecting a transition from the laminar flow (Lee, Garimella, & Liu, 2005).

A three-dimensional model has been developed in order to investigate the conjugate heat transfer in a microchannel heat sink. The development of the velocity and temperature field was considered, and the approximation of fully developed flow was eliminated. Due to the combined of convection-conduction effects in the three-dimensional setting, the unusual heat transfer pattern was obtained. As a result, the average channel wall temperature along the flow direction was nearly uniform except in a region that near the channel inlet, were founded that a very large temperature gradient. (Fedorov & Viskanta, 1999)

A three-dimensional numerical simulation of the laminar flow and heat transfer of water in silicon microchannel with non-circular cross-sections were perform. To discretize the governing equation, the finite volume method was used. As a result, inside a microchannel with the sizing of hydraulic diameter of tens of micrometer of liquid flow, the Navier-Strokes and energy equations and the no-slip boundary condition based on the continuum assumption are valid and can be used for more investigation on predicting the flow and heat transfer characteristic with reasonable accuracy. Other result shows for the microchannel simulated the heat transfer intensity of triangular microchannel much less than trapezoidal microchannel, indicationg the great effect of geometric condition in microchannel system. For the increasing of Reynolds number, the fully developed region of Nusselt number is increased to.(Li, Tao, & He, 2006)

The experimental study of the full development and heat transfer in rectangular microchannel were performed. The study was to explore the theoretical collaboration to predict the fluid flow and heat transfer characteristic in microchannel based on the conventional sized channel. 10 different rectangular microchannel with hydraulic diameter around 155 to 580µm and aspect ratio of 0.25 – 3.8 with Reynolds number ranged from 30 to 2500 investigated on flow resistance and thermal behavior of the laminar flow. The experiment was conducted by using FC770 and deionized water. The conventional Poiseuille flow theory was matched up with the single-phase laminar friction factor in the microchannel. The test apparatus consists of the pressure tank, compressed nitrogen gas supply, micro annual gear pump, filter, two Coriolis mass flowmeters, the test section in which 10 different microchannels is arranged, several valves to regulate the flow rate, recovery tank, and instrumentation. A pressure tank that stainless-steel type with 40 liters holds a capacity of the working fluid (FC770 and deionized water). The test section consists of 10 different microchannel. As a result, they verified that the critical Reynolds number was increased from 1700 to 2400 with the decreasing of the aspect ratio from 1.0 to 0.25 in a rectangular microchannel (Kim, 2016).

Only for the large-sized channel were valid for some of the results of the experiment and pressure drop through the microchannel evidence. For hydraulic diameter less than 1mm, it's not applicable. It's also found that the Reynolds number for the transition is lower than the expected result. The experimental result of the laminar to turbulence in microchannel been elaborate by using Obot-Jones model for large sized model. The model was etched on the silicon wafer, with the shape of the microchannel that trapezoidal, hexagon and rectangular was considered. They claim that critical Reynold number takes place in a range of 300 to 2000. As result of Obot analyze, they realize that for the less than 1000 Reynolds number, the critical Reynold number are not strong experimental evidence. As the conclusion, using Obot-Jones method, they verify that for hydraulic diameter 40 μm and above, its applicable to predict the laminar to turbulence flow transition (Morini, 2004).

An investigation study of the behavior of the flow transition in the rectangular microchannel by using numerical simulation. Three models were adopted, namely a γ-Reθt transition model, shear stress transport (SST) model and laminar model. The simulation was conducted using ANSYS CFX and the result was compared to the conventional one. The effect of length to diameter ratio was studied on the critical Reynolds number were study. As a result, based on the 3-model flow that been tested, only γ-Reθt transition model capture the range of the Reynold number away from the conventional based on the experiment data. For the ratio of length to diameter more than 100, transition occurs in Reynolds number of 2000 to 2500, but the length to diameter ratio has no significant effect on the critical Reynolds number. It's also been suggested to eliminate the influence of the entrance effect (Jian, Li, & Zhu Zhibing Zhi and Tao, 2017).

A single-phase flow pressure drops and heat transfer in rectangular metallic microchannel were investigated using FLUENT 14.5 in numerical simulation. A single channel with a hydraulic diameter of 0.561 mm as one of the configuration simulated. A multichannel configuration consists of inlet and outlet manifold and 25 channels with a hydraulic diameter of 0.409 mm. The result of single-channel configuration valid only for water while multichannel configuration valid using experimental data of R-134a refrigerant. As result, the transition from laminar to turbulent occur on 1600 to 2000 Reynolds number. (Sahar et al., 2015)

An investigation of water in smooth and rough silicon microchannel were conducted. By using water as testing fluid, the hydraulic diameter used to range from 153 μm to 191 μm. The rectangular roughness element mounted on the wall were 50 μm high and wide. The field measure from Reynold number 100 – 2300. The velocity profile was conducted using microscope particle image velocimetry (micro-PIV) shows that transition occurred between 900 – 1100. As suggestion, the fluid flow becomes developed fully turbulence for Reynold number more than 1400 at the rough microchannel. (Zhu, 2006)

The friction factor in the transition region flow water flow in minutes and microtubes were investigated. The single-phase water flow was performed for twelve stainless-steel tubes diameter ranging from 2083 μm to 337 μm. As a result, the transition from laminar to turbulence is 1300 to 4000 Reynolds number. The Reynold number range for transition flow become narrower with decreasing tube diameter. (Ghajar, Tang, & Cook, 2010)

The liquid flow in microchannel was investigated in form of experiment and numerical method by using hydraulic diameter from 244 μm to 974 μm at a range of Reynold 230 to 6500.

As result, they agreed on the argument that developing fully turbulence flow is retarded in the microchannel and critical Reynolds number is approximately at 2000 (Liu & Garimella, 2004)

Moreover, the surface roughness effect studies on the flow behavior and heat transfer characteristic in a circular microchannel with 0.4 mm diameter and 10 mm length. the surface roughness is 0.86, 0.92,1.02 µm with a range of Reynolds number starting at 150 to 2800. As a result, the roughness is significant on effecting the flow circulation in the microchannel. the critical Reynold occur at 1500. For heat transfer properties, increasing Reynold number is increased the Nusselt number, higher roughness is contributed to higher Nusselt's number. (Yuan, Tao, Li, & Tian, 2016)

Three-dimensional fluid flow and heat transfer in a microchannel heat sink are analyzed numerically using water as cooling fluid. 1 cm^2 silicon wafer was used as heat sink. Microchannel consist of 180 µm depth and 57 µm width and separated with 43 µm wall. The SIMPLE algorithm is used to solve governing equation. Increasing Reynolds number increases the length of the developing region (Qu & Mudawar, 2002). Table 2.1 and Table 2.2 shows the summarizes of critical Reynolds number determined from previous works.

Table 2.1: Summary reference on critical Reynolds number for water as testing fluid

Reference	**Geometry**	**Hydraulic Diameter**	**Re range**	**Critical Re**	**Conclusion**
(Pfund et al., 2000)	Rectangular	252 - 973 µm	60 - 3450	1700 – 2200	Transition value was lower than conventional critical Reynolds number
(Wu & Cheng, 2003)	Trapezoidal	25.9 - 291.0 µm	100 – 3000	1500 - 2000	They prove that Navier-stokes equation that follows non-slip condition was still applicable for deionized water flow in smooth silicon microchannel having in 25.9 µm hydraulic diameter
(Dirker et al., 2014)	Rectangular	0.57, 0.85, 1.05 mm	300 - 3000	1800 – 2000	Critical Reynold number and the transition behavior influences by the inlet type

(Lee et al., 2005)	Rectangular	318 - 903 µm	300 - 3500	1500 – 2000	Transition occur at Reynolds number 1500 - 2000
(Kim, 2016)	Rectangular	155 - 580 µm	30 - 2500	1700 – 2400	Verified that the critical Reynolds number was increased from 1700 to 2400 with the decreasing of the aspect ratio from 1.0 to 0.25 in a rectangular microchannel
(Ghajar et al., 2010)	Circular	337 - 2083 µm	Not Stated	1300 - 4000	Reynold number range for transition flow become narrower with decreasing tube diameter
(Sahar et al., 2015)	Rectangular	0.409, 0.561 mm	Not Stated	1600 – 2000	transition from laminar to turbulent occur on 1600 to 2000 Reynolds number
(Zhu, 2006)	Rectangular	153 - 191 µm	100 - 2300	900 – 1100	the fluid flow become develop fully turbulence

					for Reynold number more than 1400 at the rough microchannel
(Liu & Garimella, 2004)	Rectangular	244 to 974 µm	230 to 6500	2000	agreed on the argument that developing fully turbulence flow is retarded in the microchannel
(Yuan et al., 2016)	circular	Diameter 0.4 mm 10 mm length	150 to 2800.	1500	The roughness is significant on effecting the flow circulation in the microchannel
(Qu & Mudawar, 2002)	Rectangular	86.58 µm	140, 700,1400	Not Stated	Increasing Reynolds number increases the length of the developing region

Table 2.2 : Summary reference on critical Reynolds number for R-134 and other testing fluid

Reference	**Geometry**	**Hydraulic Diameter**	**Re Range**	**Critical Reynolds**	**Conclusion**
(Hrnjak & Tu, 2007)	Rectangular	69.5 - 304.7 µm	112 - 9180	2150 – 2290	Surface roughness become low, critical Reynold number and friction factor significant toward conventional value
(Morini, 2004)	Trapezoidal, Hexagon, Rectangular	Not Stated	300 - 2000	Not Stated	Verify that for hydraulic diameter 40 µm and above, its applicable to predict the laminar to turbulence flow transition
(Jian et al., 2017)	Rectangular	Use Length to Diameter	Not Stated	2000 – 2500	length to diameter ratio has no

		range more than 100 µm			significant effect on the critical Reynolds number

CHAPTER 3

METHODOLOGY

3.1 Introduction

This chapter outline the design drawing, meshing and boundary condition used to study the critical Reynolds number of water flow inside a microchannel. All details, method used, and equation is described on this chapter.

As to achieve the objectives of this research, the tasks that need to be completed is shows in Table 3.1 and Table 3.2 shows below

Table 3.1: The Gantt Chart of PSM I Tasks

No.	Task	Week													
		1	2	3	4	5	6	7	8	9	10	11	12	13	14
1	Research Title Selection														
2	Internet and Library Search														

3	Preparation of Chapter 1														
4	Preparation of Progress Report 1														
5	Submission of Progress Report 1														
6	Preparation of Chapter 2: Literature Review														
7	Data Collection: a. Critical Reynolds number b. Model of rectangular microchannel														
8	Preparation of Chapter 3: Methodology														
9	Edit PSM 1 Report														

10	Prepare Slides for Presentation on PSM 1 Seminar														
11	Submission of PSM 1 Report														

Table 3.2 : The Gantt Chart of PSM II Tasks

No.	Task	Week													
		1	2	3	4	5	6	7	8	9	10	11	12	13	14
1	Spread the research question														
2	Fluent 6.1 - Mesh Independent Test														
3	Fluent 6.1 - Validation														
4	Fluent 6.1 - Temperature distribution and Nusselt														

5	Fluent 6.1 - Velocity profile setup														
6	Record and analyse data														
7	Preparation of Chapter 4; Data and Result														
8	Preparation of Chapter 5; Conclusion														
9	Writing full thesis														
10	Prepare slides for presentation														
11	Seminar PSM 2														
12	Submission of PSM 2 report														

While, Figure 3.1 shows the flow chart about the methodology of the project. It has been done from the beginning until finishing. This is to make sure that the work has been done smoothly by following the systematic and true path.

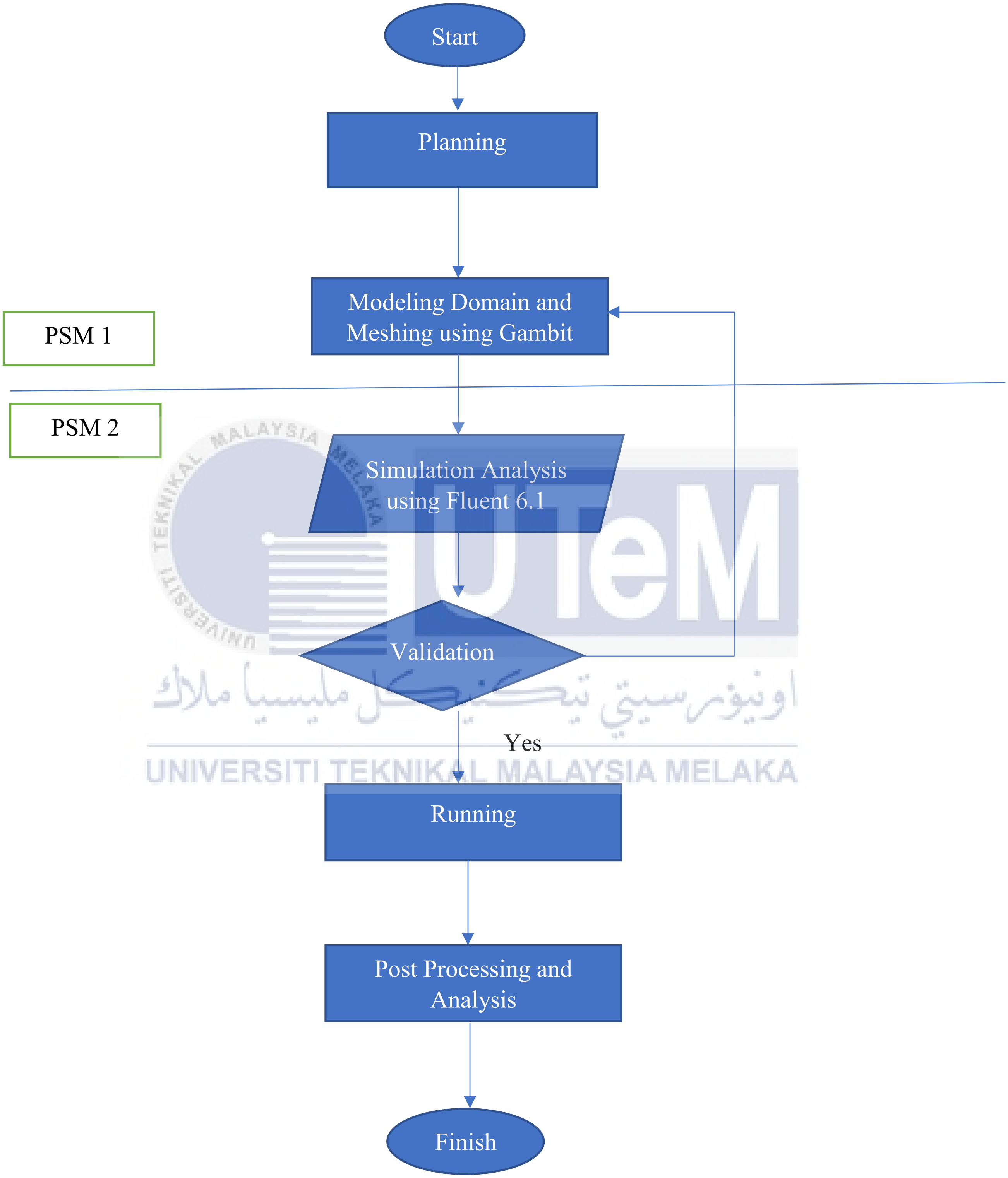

Figure 3.1 : Flow Chart of Methodology

3.2 Model Domain

To study the velocity profile of water flow inside a microchannel, the model of microchannel is developed. Gambit 2.4.6 software is used to model the rectangular shape microchannel Figure 3.2 shows the illustrated structure of the rectangular microchannel. The hydraulic diameter of the channel is 86.58 µm and copper is used as a solid substrate.

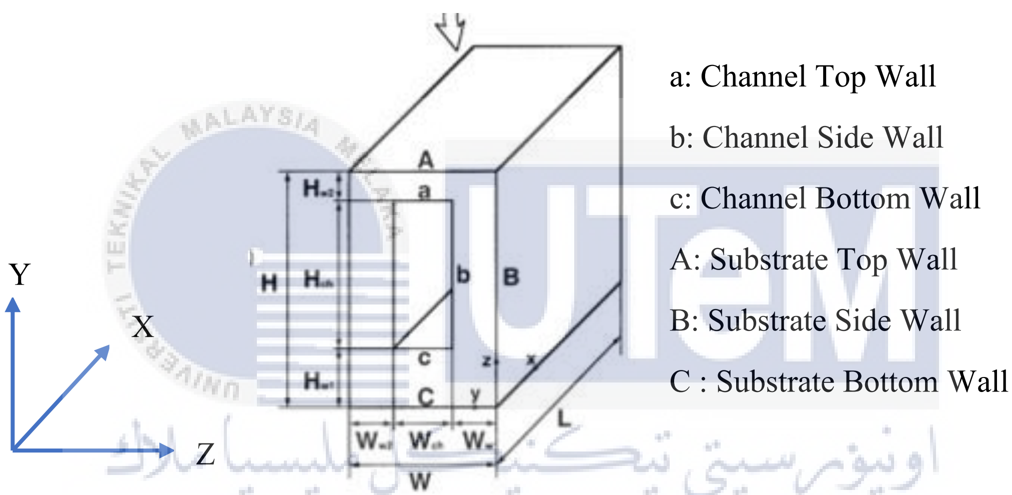

Figure 3.2 : Schematic of rectangular microchannel (Qu & Mudawar, 2002)\

Figure 3.3 shows model of rectangular microchannel using Gambit 2.4.6 software. The dimension labelling of the rectangular microchannel follow the is the same as previous work (Qu & Mudawar, 2002), as shows in Figure 3.2 and the dimensions shows in Table 3.3. The X -axis is the length of the channel, Y-axis is the height and Z-axis is the width of the channel.

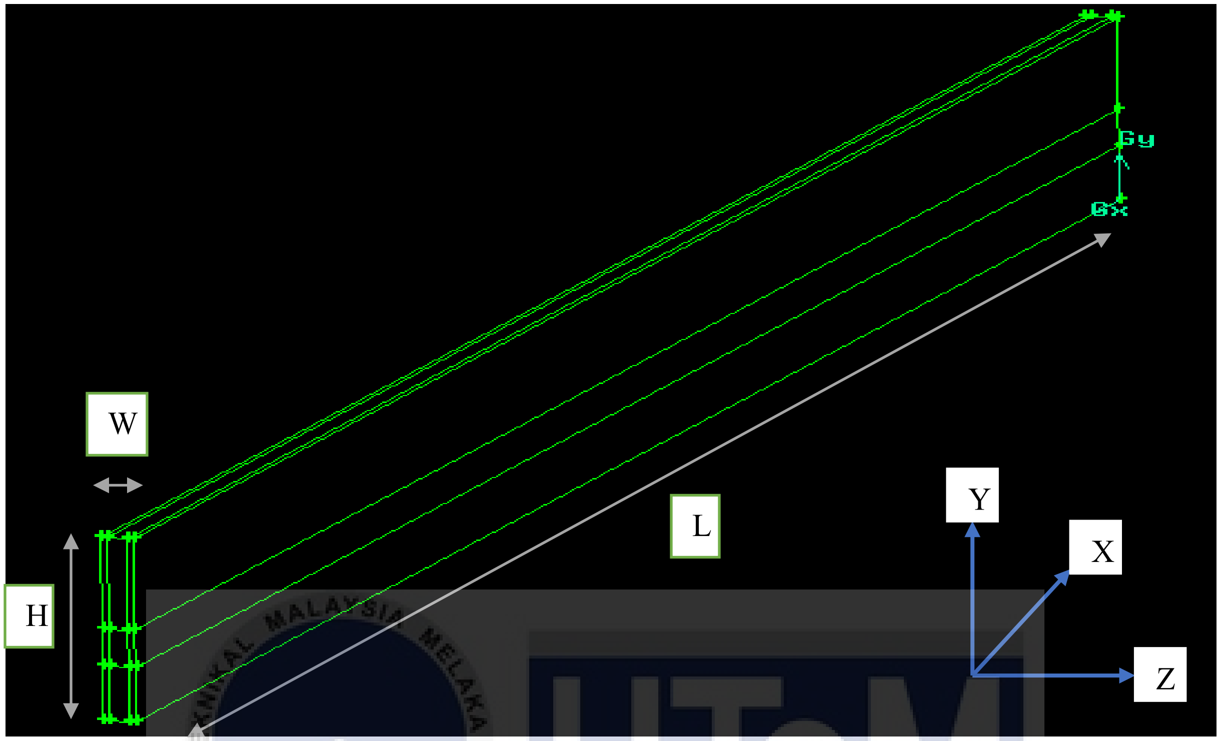

Figure 3.3 : Schematic of rectangular microchannel using Gambit

Table 3.3: Dimension of unit cell of microchannel

H_{ch}	H_{w1}	H_{w2}	W_{ch}	W_{w1}	W_{w2}	L	D_h
180 µm	270 µm	450 µm	57 µm	21.5 µm	21.5 µm	10 mm	86.58 µm

3.3 3D Meshing

The process after drawing the model is to complete the meshing of the model, the 3D meshing must be done. The node number is determined for every surface of the rectangular microchannel from the inlet to the outlet along the X-Y plane and X-Z plane. The meshing show in Figure 3.4 is done using also Gambit 2.4.6 software. The volume meshing element option Hex map is use. Hex map type creates a regular, structural grid of hexahedral mesh elements. Table 3.4 shows the grid system for every surface on the 3D model follow the schematic label on Figure 3.4. A non-uniform grid arrangement in the x-direction with a large number of grid point near the channel inlet and outlet is used to resolve the flow developing region.

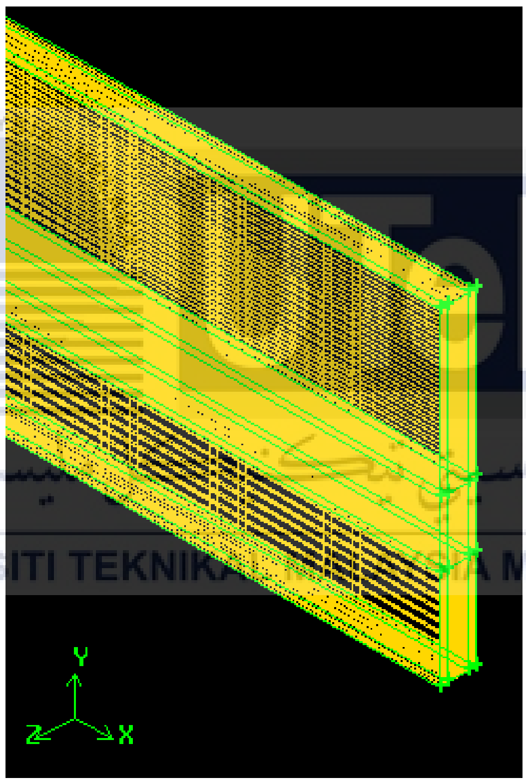

Figure 3.4 : Meshing Domain

Table 3.4: Grid System

Label	H_{w1}	H_{w2}	H_{ch}	W_{w1}	W_{w2}	W_{ch}	L
Nodes	20	20	30	5	5	20	150

After this meshing process, running process is done simulation using FLUENT 6.1 software. The boundary condition and thermal properties is set on the model.

3.4 Boundary Condition

In the boundary condition, the model is divided into 2 zones named as boundary type and continuum types. The continuum type is divided into 2 types as shows in Table 3.5. For boundary types, as shows in Table 3.6.

Table 3.5: Continuum type

Name	Type
Water	Fluid
Copper	Solid

Table 3.6: Boundary Type

Name	Type
Inlet	Wall
Outlet	Wall
TopWall	Wall
BottomWall	Wall
SolidFluid	Interface

All unit cell are chosen as unitary domain for this study. In the condition of hydraulic boundary, the velocity is zero at all boundary other than channel inlet and outlet. At channel inlet, a uniform velocity is applied.

$$u = \frac{Re\,.\mu_f}{d_h}\,,\ v = 0\,,\ w = 0$$

For $x = 0$, $W_{w1} \leq y \leq W_{w1} + W_{ch}$, and $H_{w1} \leq z \leq H_{w1} + H_{ch}$

At the channel outlet, the flow is fully developed.

$$\frac{\partial u}{\partial x} = 0,\ \frac{\partial v}{\partial x} = 0,\ \frac{\partial w}{\partial x} = 0,$$

For $x = L$, $W_{w1} \leq y \leq W_{w1} + W_{ch}$, and $H_{w1} \leq z \leq H_{w1} + H_{ch}$

For thermal boundary condition, all the boundaries of the solid region except the substrate top wall, where a constant heat flux is assumed are applied as adiabatic boundary condition.

$$-k_s \frac{\partial T}{\partial z} = q'', \quad \text{for } 0 \leqslant x \leqslant L,\ 0 \leqslant y \leqslant W,\ \text{and } z = H.$$

The liquid temperature is constant inlet temperature at the channel inlet.

$T = T_{in}$

The local Nusselt number Nu is defined as

$$Nu = \frac{q'' d_h}{k_f (T_{s,\Gamma} - T_m)},$$

3.5 Model Surface

The model surface line of the substrate top wall, fluid bulk(middle) can be identify by using the all illustration on Figure 3.5 in order to get the temperature distribution on that line for validation and Nusselt number. Figure 3.6 shows the surface line at x=1 mm, x= 3 mm, x= 7 mm and x= 9 mm and are used it for obtaining the velocity profile.

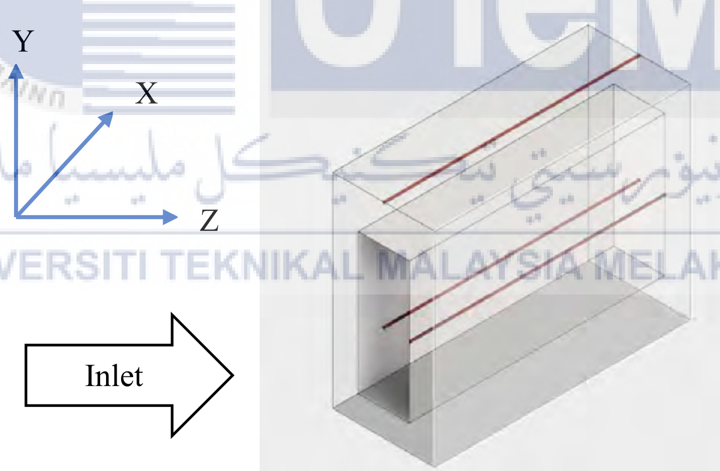

Figure 3.5: Surface line of Substrate Top Wall, Channel Fluid Bulk and Channel Side Wal

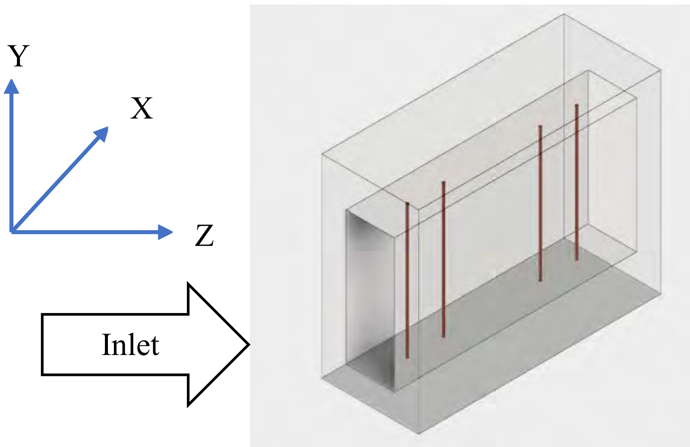

Figure 3.6: Surface line of in the channel at x=1mm, x=3mm, x=7mm and x = 9 mm

Figure 3.7 shows the surface planes on the channel top wall, channel side wall and channel bottom wall for the temperature distribution. Figure 3.8 shows the surface on x-y plane at the middle and substrate side wall and Figure 3.9 shows surface on y-z plane at the x=0, x=5 mm and x=10 mm. Both for these figures are used in contributing the temperature distribution.

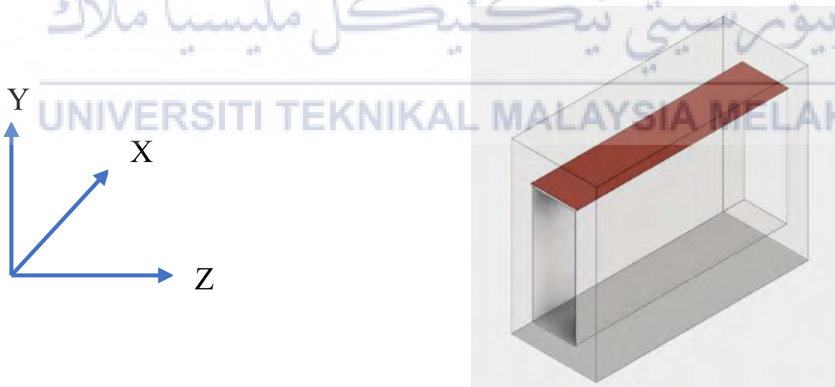

(a)

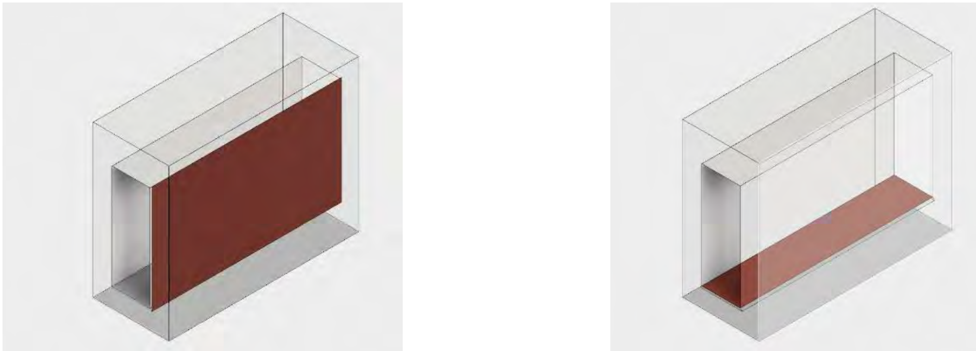

(b) (c)

Figure 3.7: Surface on plane (a) Channel Top Wall (b)Channel Side Wall (c) Channel Bottom Wall

(a) (b)

Figure 3.8: Surface on x-y plane (a) Middle plane (b) Substrate Side Wall

(a)

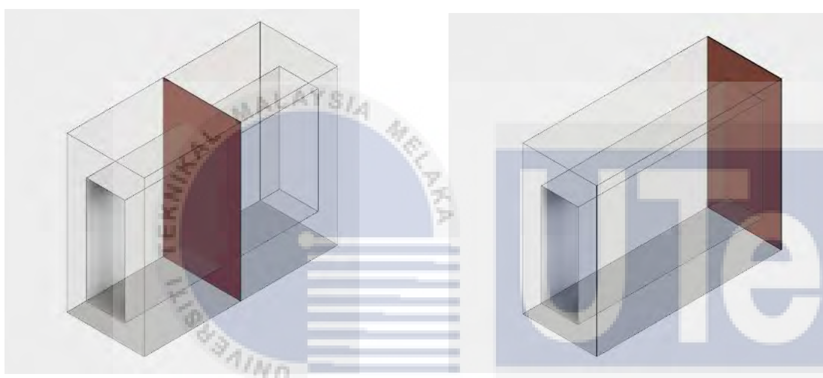

(b) (c)

Figure 3.9: Surface on y-z plane (a) x=0 (b) x=5 mm (c) x=10mm

3.6 Thermal Properties

The thermal properties of water and copper are shows in Table 3.7 and Table 3.8.

Table 3.7: Thermal properties of water

Density (kg/m^3)	998.2
C_p (specific heat)(j/kg.k)	4182
k, Thermal Conductivity (w/m.k)	0.6
μ, Viscosity (kg/m.s)	0.001003

Table 3.8: Thermal properties of copper

Density (kg/m^3)	8978
C_p (specific heat)(j/kg.k)	381
k, Thermal Conductivity (w/m.k)	387.6

CHAPTER 4

DATA AND RESULT

4.1 Introduction

In this section, numerical analysis is performed for the rectangular microchannel and result are presented. The validation is prepared mesh independent test, temperature distribution, the velocity profile and Nusselt number.

4.2 Mesh Independent Test

To reduce time and iteration process, mesh independent test is used to get the best profiles of mesh. The number of cells on the channel side wall is varied from 270000 to 360000. A meshing is considered as grid independent if the average Nusselt number remains constant although the number of cells increases. Based on Figure 4.1, the average Nusselt number at 270000 numbers of cells can be chosen because the average Nusselt number is still constant although the numbers of cells increase.

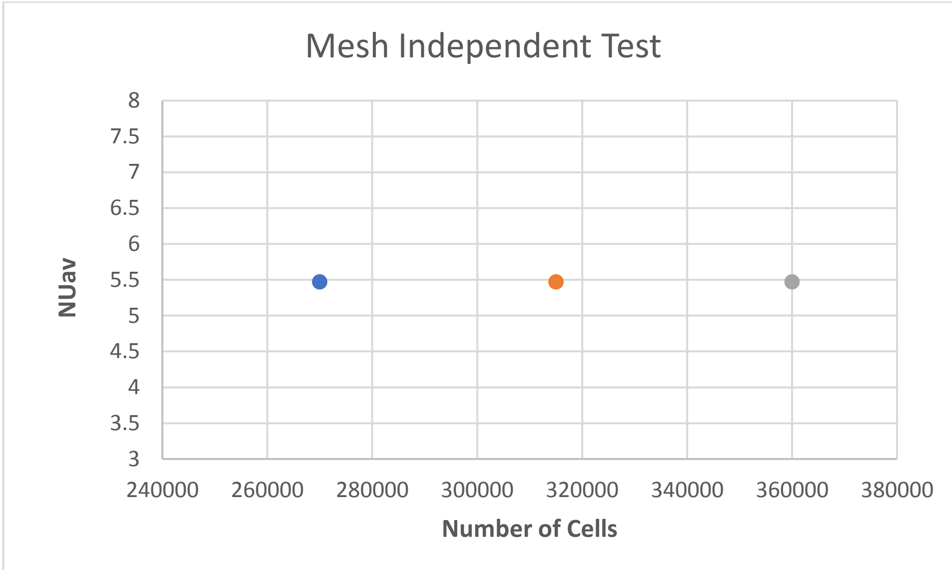

Figure 4.1 : Mesh Independent Test

4.3 Validation

The validation process is a process to make sure that simulation is valid. Data that obtained from FLUENT 6.1 software is analyzed. The average temperature of channel top wall and fluid bulk are plotted in Figure 4.2.

Figure 4.3 shows the Nusselt number for channel side wall and substrate top wall. The result ware obtained from the equation based on the result of average heat flux from channel side wall and channel top wall and the average temperature from fluid bulk and channel side wall.

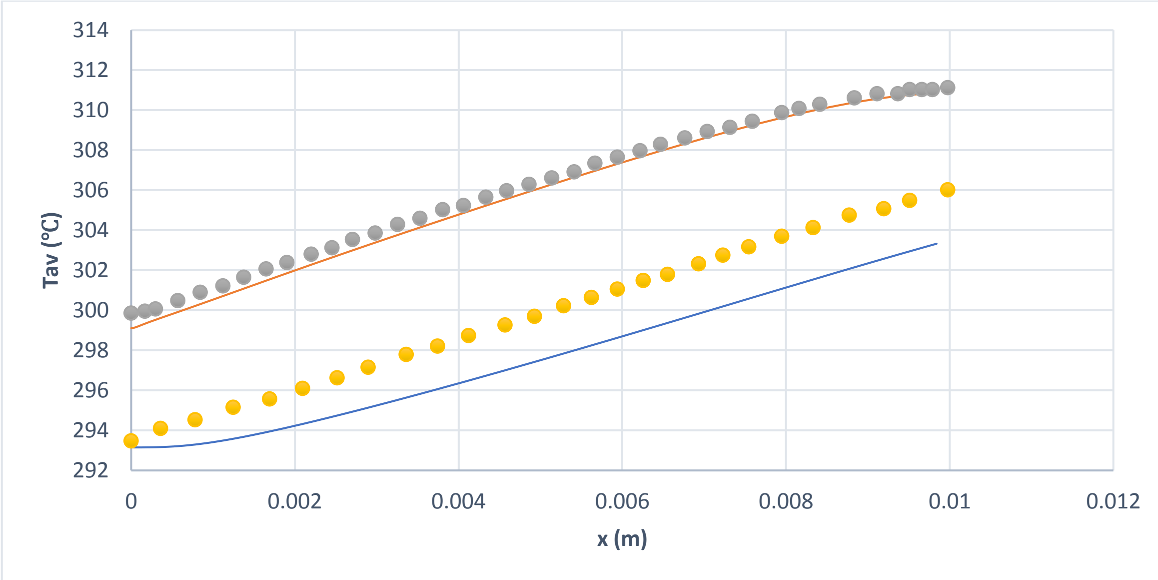

Figure 4.2: Average Temperature along the x-direction

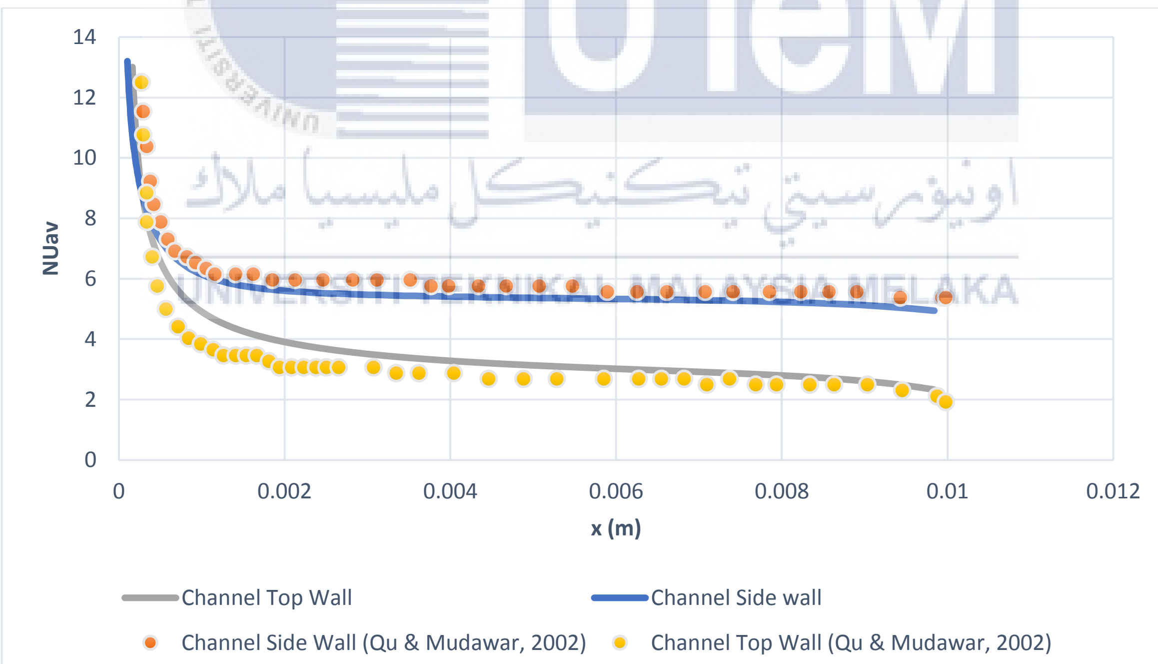

Figure 4.3 : Average Nusselt number along x-direction

Regarding from illustration shows in Figure 4.2, the different average temperature between result obtained and (Qu & Mudawar, 2002) was about only 0.33% at most at all x-direction at the substrate top wall. However, at fluid bulk, the temperature different becomes 0.66%.

At Figure 4.3 for the Nusselt number, only 7.88% different at most detected on the channel side wall along the x-direction. It a different story at channel top wall because the highest Nusselt number different approximately 11.90%.

4.4 Velocity Profile

Figure 4.4 show the velocity profile at Reynolds number 1000, 1250 and 1500 respectively. All these figures show the development of average velocity profile at x= 7mm and x=9mm. At this position, the region is already a fully developed laminar flow. At this fully developed region, each fluid particle moves at a constant axial velocity along a streamline and the velocity profile remains unchanged in the flow direction. Although at line x= 1mm and x=3mm average velocity profile is flatter and fuller, it is not considered to be turbulence flow because of the developed is in the entrance region. However, with the increases of the Reynolds number, the pattern of the velocity profile become toward fuller or flatter. Which mean if the Reynolds number is much higher than 1500, the flow is attempted to become turbulence flow. Figure 4.5 show the development of velocity profile a Re = 1000. Its shows that the fully developed flow has no change in velocity profile.

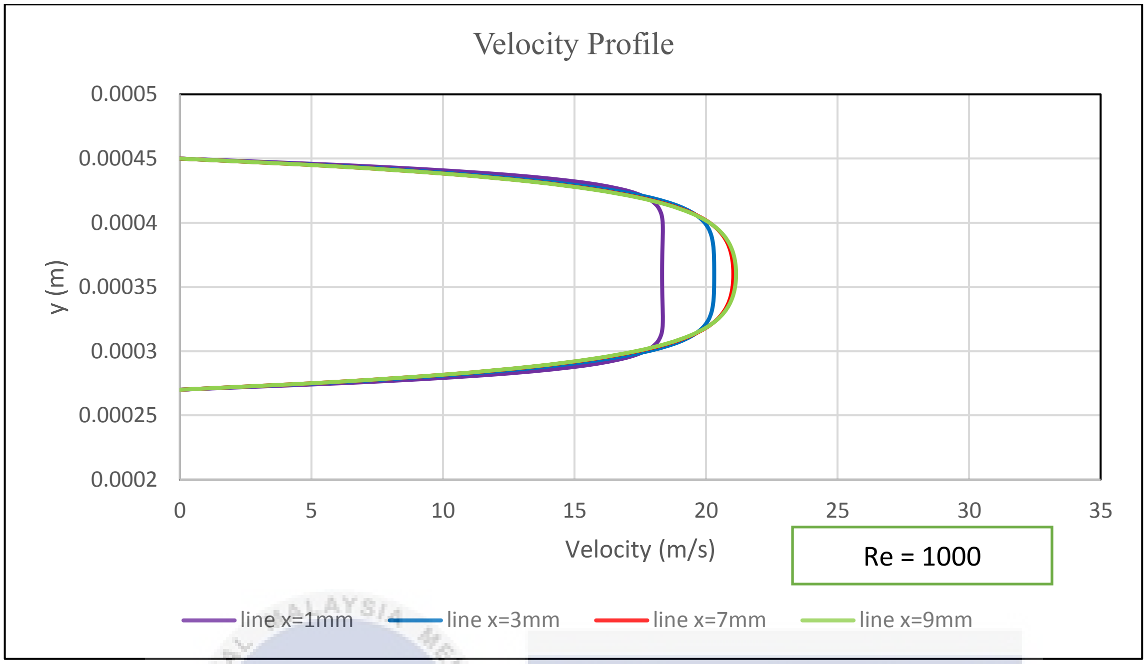
Velocity Profile
0.0005
0.00045
0.0004
0.00035
0.0003
0.00025
0.0002
y (m)
0
5
10
15
20
25
30
35
Velocity (m/s)
Re = 1000
line x=1mm
line x=3mm
line x=7mm
line x=9mm

(a)

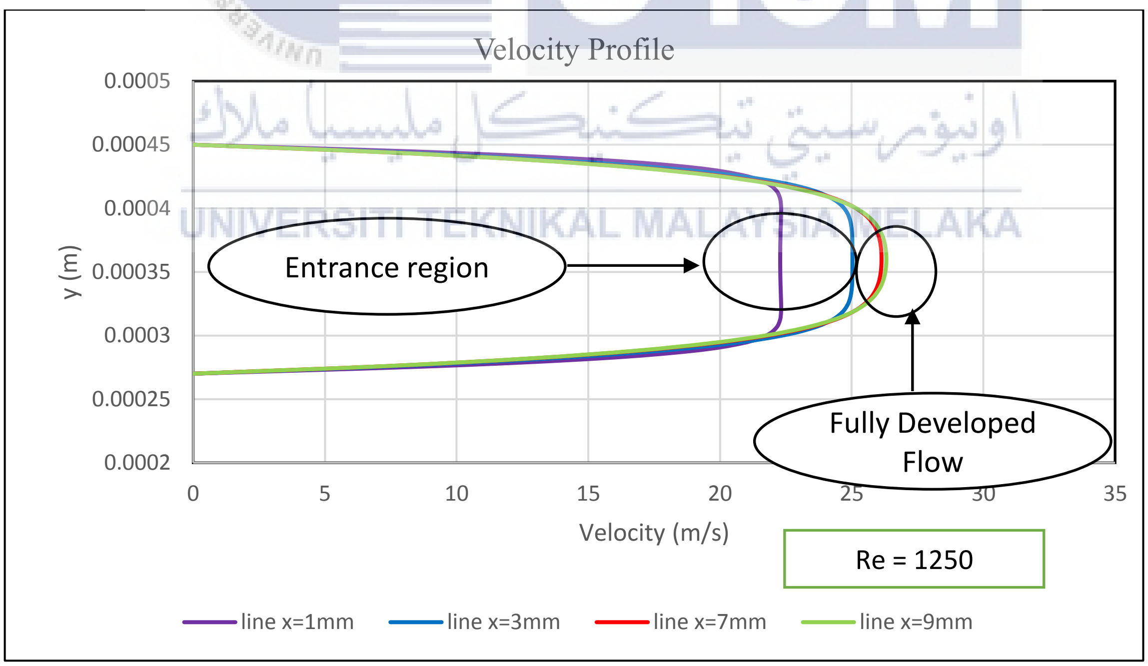
Velocity Profile
0.0005
0.00045
0.0004
0.00035
0.0003
0.00025
0.0002
y (m)
Entrance region
Fully Developed
Flow
0
5
10
15
20
25
30
35
Velocity (m/s)
Re = 1250
line x=1mm
line x=3mm
line x=7mm
line x=9mm

(b)

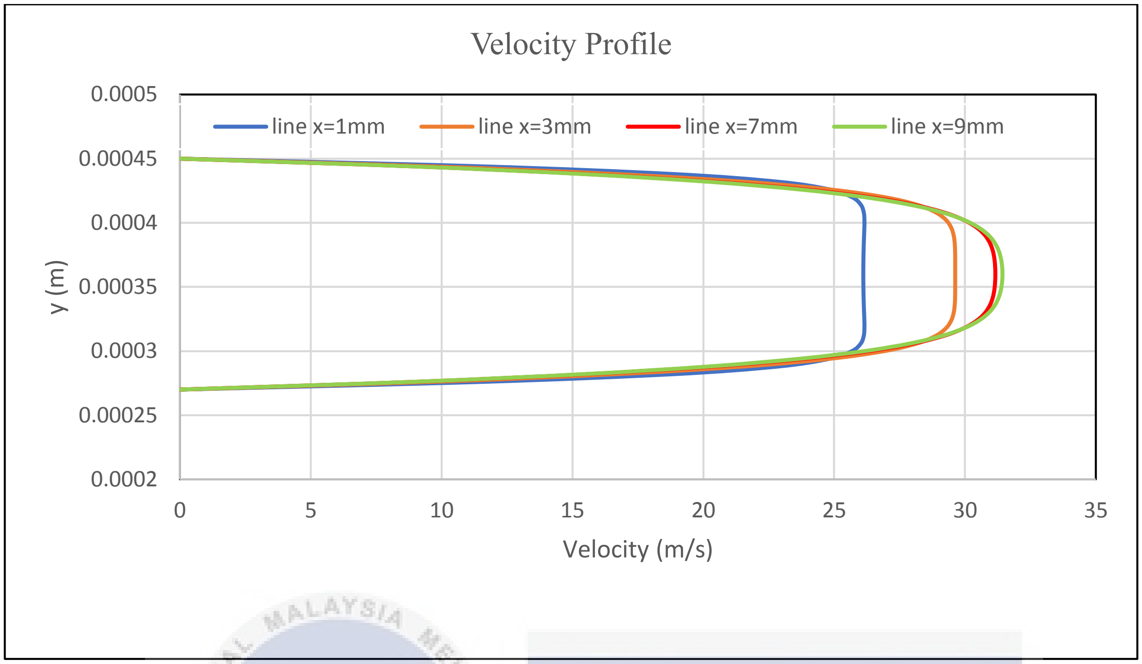

(c)

Figure 4.4: Velocity profile at (a) Re = 1000, (b) Re = 1250, (c) Re 1500

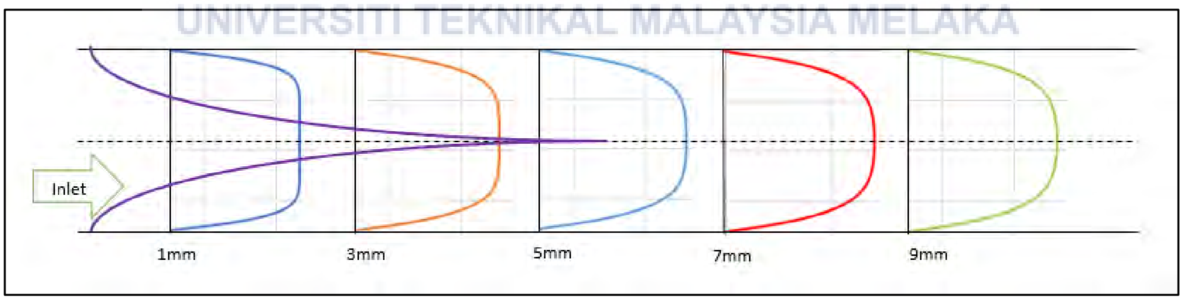

Figure 4.5: Development of the velocity profile in the microchannel for Re = 1000

4.5 Temperature Distribution

Figure 4.6 shows the average temperature at the channel top wall and channel bottom wall at the various Reynolds number. Its shows the highest temperature occur at the channel top wall at Reynolds number of 1000.

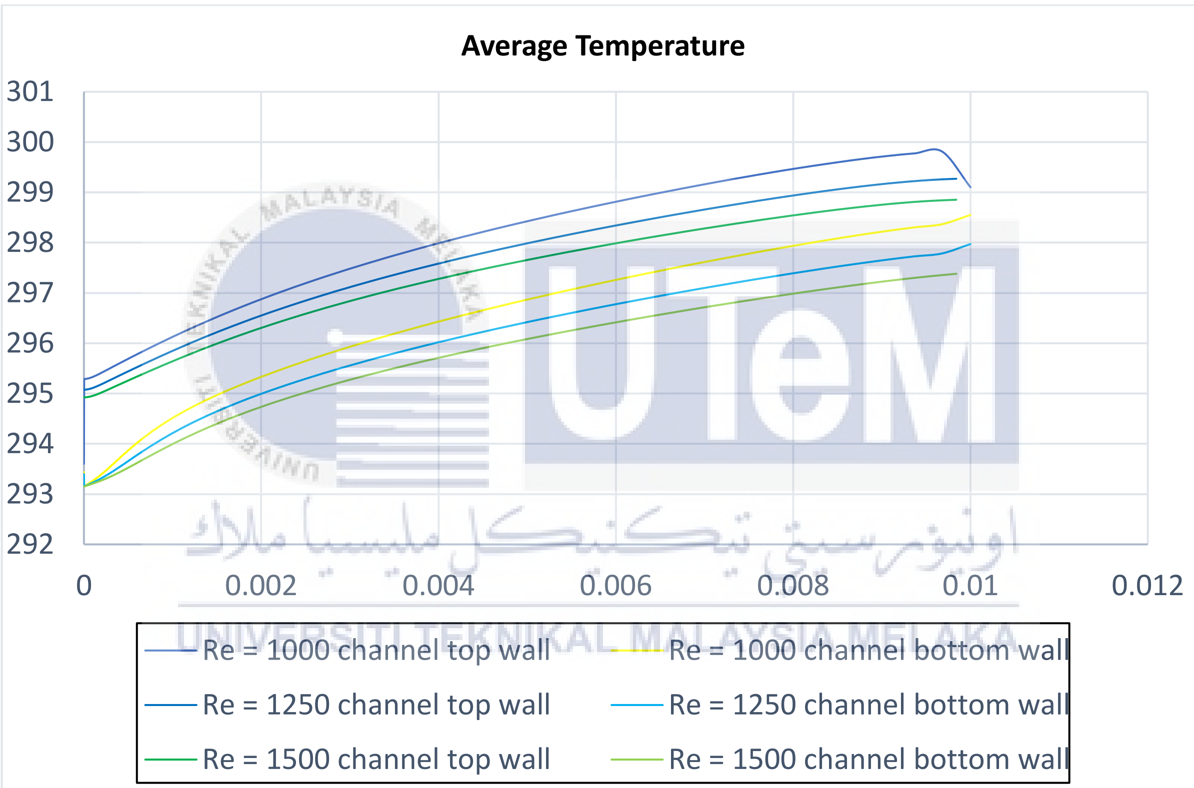

Figure 4.6: Average Temperature

Figure 4.7 shows the illustration of temperature distribution on several x-y planes namely the channel top wall and channel bottom wall. Some feature is readily observed. From the distribution temperature of constant temperature contour lines, along with the longitudinal x-direction, the temperature gradient decreases from the channel inlet to outlet for both channel top and a bottom wall. The linear temperature rise is a good sign for the studies because of the constant heat flux assumed at substrate top wall. The temperature nearly constant among the transverse y-direction. The temperature also becomes lower from channel top wall to the channel bottom wall.

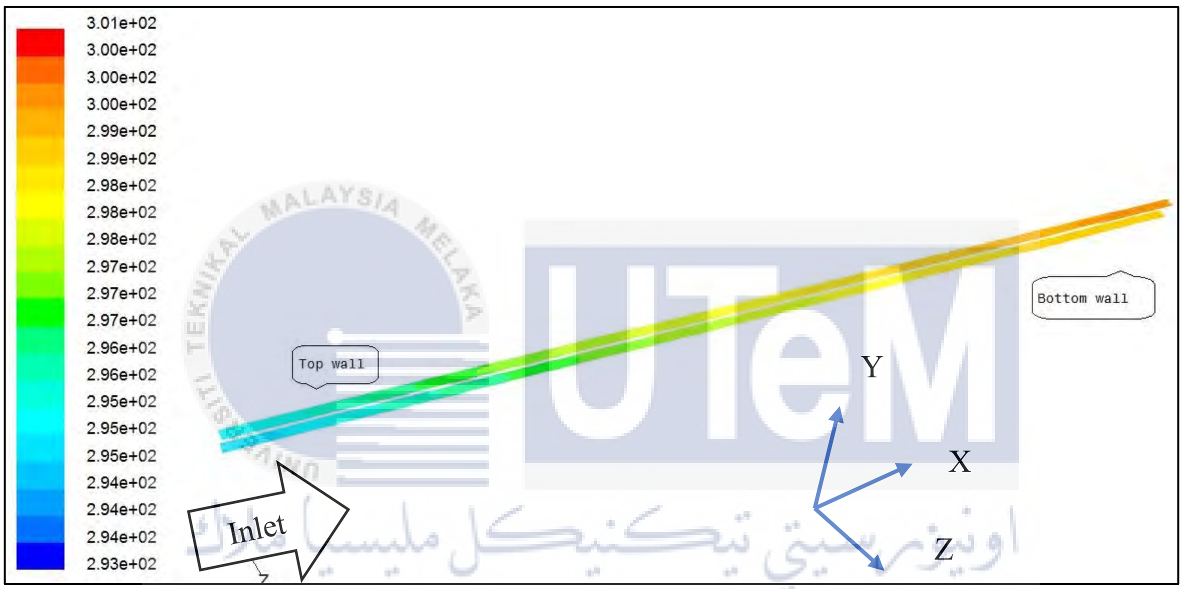

Figure 4.7: Local temperature distribution in the x-z plane at channel top wall and bottom wall

Figure 4.8 and Figure 4.9 show the temperature distribution on the x-y planes at the middle plane and side wall plane. From the Figure 4.8, the shape channel from the inlet to outlet become clearly visible due to the higher temperature gradient difference between the fluid and solid. Copper is a high thermal conductivity solid substrate, so the temperature gradient of copper is much smaller compare with water. Other than that, both figures confirmed that the temperature is approximately constant in the transverse y-direction in the solid. Additional, the thickness and the material of the channel significant on heat transport. This shows that the region above the channel is high-temperature gradient as compared to the channel below at each y-z cross-section.

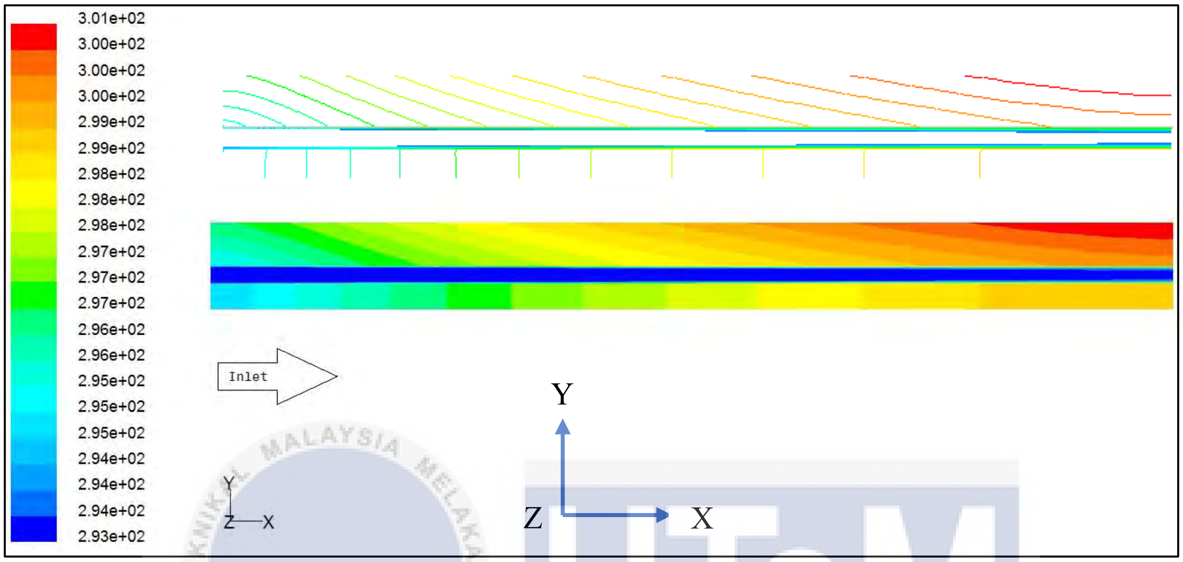

Figure 4.8: Local temperature distribution in the x-y plane middle plane

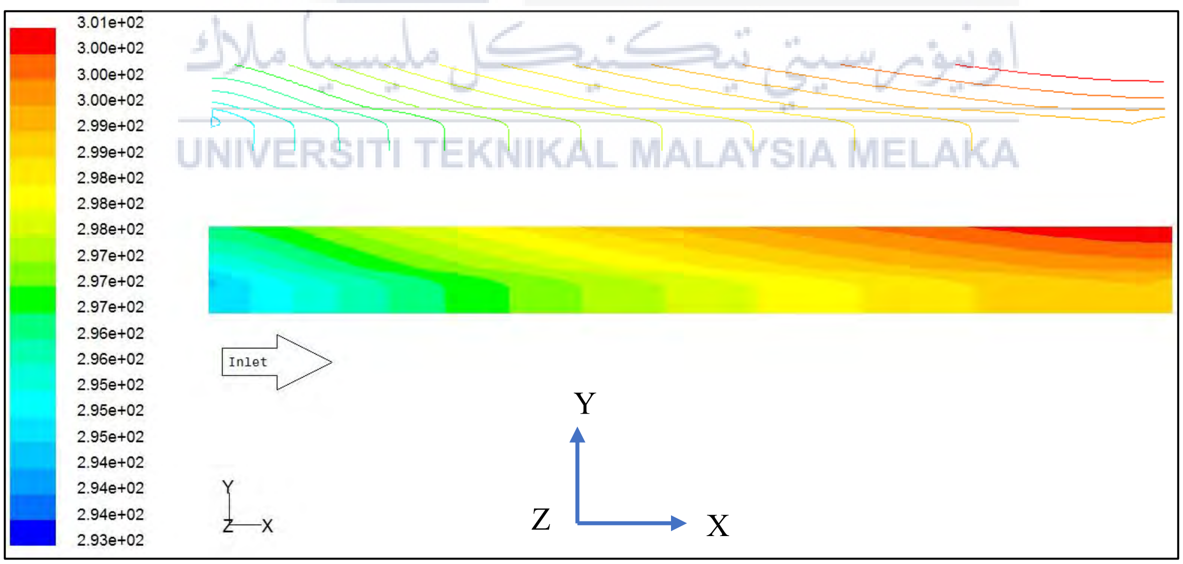

Figure 4.9: Local temperature distribution in the x-y plane side wall

Temperature distribution at three cross sections along longitudinal x-direction shows in Figure 4.10. At the inlet (x=0), the fluid temperature becomes uniform. The temperature gradient on solid substrate also smaller compare to fluid. However, at the middle plane (x=5mm) and outlet (x=10mm), the temperature changes due to development of thermal boundary layer.

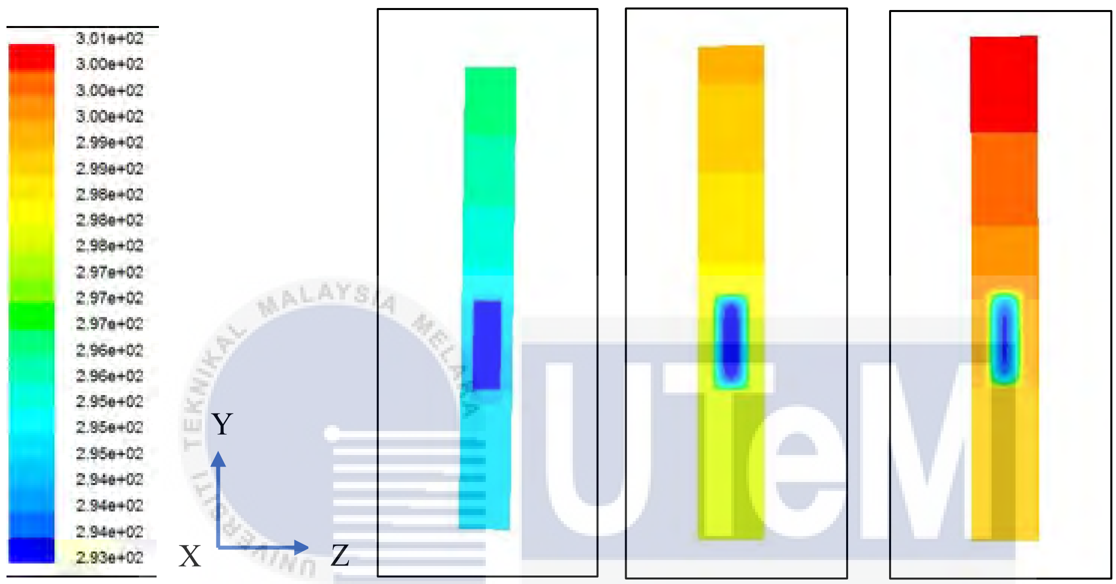

(a)x=0 (b) x= 5mm (c) x = 10mm

Figure 4.10: Local temperature distribution in y-z plane

4.6 Nusselt Number

Figure 4.11 and Figure 4.12 illustrates the average Nusselt number along with the longitudinal x-direction on channel side wall and channel top wall with its entry length. With the increases of Reynolds number, the average Nusselt number also increases. It shows that the thermal developing region is larger than the channel length because of the maintained trend through the outlet. This proves at the high Reynolds number, the fully developed condition cannot be archived inside the microchannel.

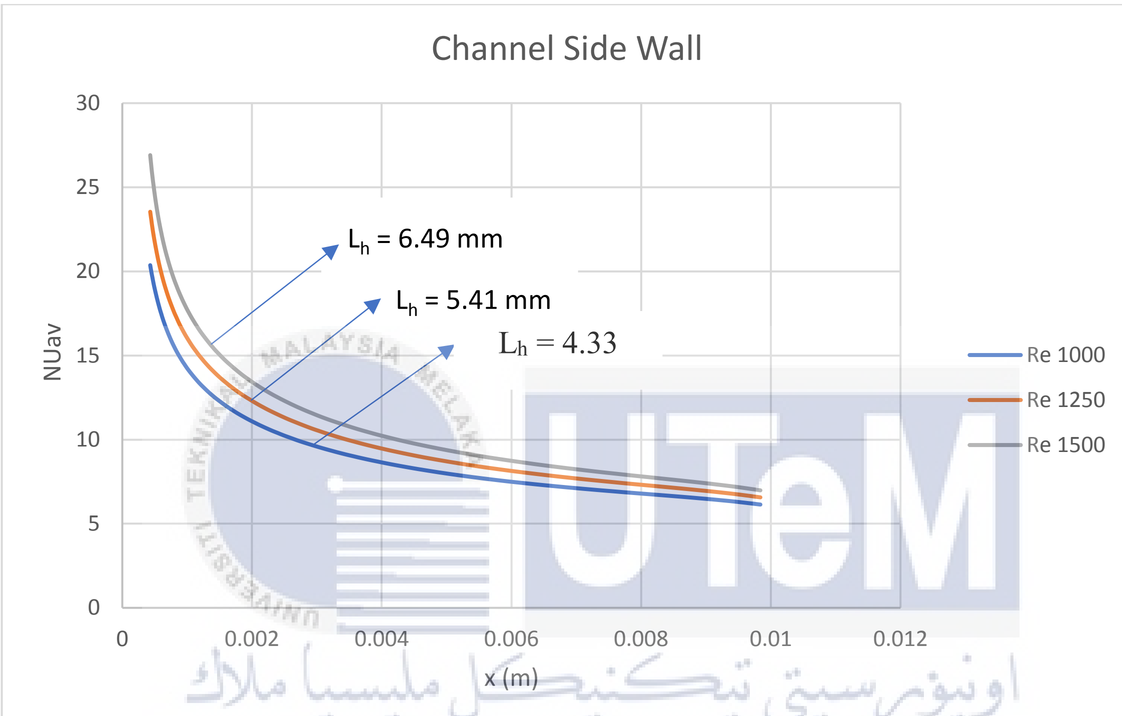

Figure 4.11: Average Nusselt number at channel side wall

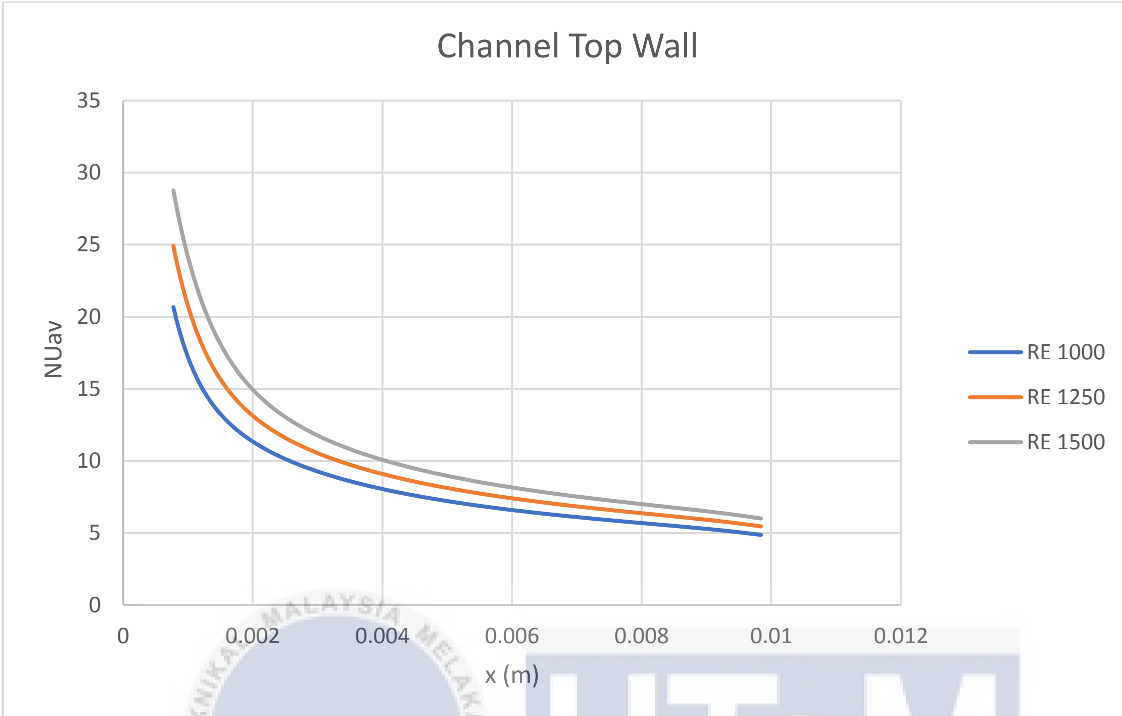

Figure 4.12: Average Nusselt number at channel top wall

CHAPTER 5

CONCLUSION

5.1 Introduction

In this chapter, result and discussion of the numerical analysis is concluded and recommended for the upcoming work. The average temperature, velocity profile and Nusselt number was obtained on this fluid flow analysis on the rectangular microchannel. The thermal conductivity on the solid substrate and cooling fluid were discussed. Not forgotten the effect of Nusselt number with various of Reynolds number. Moreover, the validity of the numerical analysis is accepted because of the different value is too small.

5.2 Conclusion

Regarding to the validation process, the highest deviation occurs at the channel top wall for the Nusselt number. The deviation is 11.90% with the comparison other paper. While for the temperature. The deviation occurs highest at the fluid bulk with the 0.66% value. This validation using the numbers of cells 270000.

Based on the average temperature distribution, the temperature rise along flow direction in solid and fluid region can be approximately linear. The highest temperature occurs at the substrate top wall above the channel outlet with the value of 301 Kelvin. However, along the transverse y-direction, the temperature at a given longitudinal distance x is nearly constant. Other that, the temperature gradient of solid substance is lower compare to cooling fluid because of the high thermal conductivity of the solid substrate.

Nusselt number much higher at near channel inlet. However, as the Nusselt getting closer to the outlet, the number approaches 5. With the increases of Reynolds number more than 1500, the average Nusselt number also increases. It is shows that the thermal developing region is larger than the channel length because of the maintained trend through the outlet. This proves at the high Reynolds number, the fully developed condition cannot be archive at larger Reynolds number inside the microchannel.

All the three figures shows the development of average velocity profile is parabolic at nearly outlet. At that line, the region is already a fully developed laminar flow. Although at nearly inlet average velocity profile is flatter and fuller, it not considers the turbulence flow because of the developed is in the entrance region. However, when the Reynolds number increase, the pattern of the velocity profile become toward fuller or flatter. Its mean that it nearly toward transitional flow. At the fully developed flow, there is no change is velocity profile pattern.

REFERENCES

Cengel, Y. A. ., & Cimbala, J. M. . (2014). *Fluid Mechanics: Fundamentals and Applications*. Retrieved from http://highered.mheducation.com/sites/0073380326/information_center_view0/index.html

Dirker, J., Meyer, J. P., & Garach, D. V. (2014). Inlet flow effects in micro-channels in the laminar and transitional regimes on single-phase heat transfer coefficients and friction factors. *International Journal of Heat and Mass Transfer*, *77*, 612–626. https://doi.org/10.1016/j.ijheatmasstransfer.2014.05.048

Fedorov, A. G., & Viskanta, R. (1999). *Analysis of conjugate heat transfer in a three-dimensional microchannel heat sink for cooling of electronic components*. *American Society of Mechanical Engineers, Heat Transfer Division, (Publication) HTD* (Vol. 364).

Ghajar, A. J., Tang, C. C., & Cook, W. L. (2010). Experimental investigation of friction factor in the transition region for water flow in minitubes and microtubes. *Heat Transfer Engineering*, *31*(8), 646–657. https://doi.org/10.1080/01457630903466613

Hassan, I., Phutthavong, P., & Abdelgawad, M. (2004). Microchannel heat sinks: An overview of the state-of-the-art. *Microscale Thermophysical Engineering*, *8*(3), 183–205.

https://doi.org/10.1080/10893950490477338

Hrnjak, P., & Tu, X. (2007). Single phase pressure drop in microchannels. *International Journal of Heat and Fluid Flow*, *28*(1 SPEC. ISS.), 2–14. https://doi.org/10.1016/j.ijheatfluidflow.2006.05.005

Jian, C., Li, H., & Zhu Zhibing Zhi and Tao. (2017). NUMERICAL SIMULATION OF FLOW TRANSITION IN A RECTANGULAR MICROCHANNEL.

Kim, B. (2016). An experimental study on fully developed laminar flow and heat transfer in rectangular microchannels. *International Journal of Heat and Fluid Flow*, *62*, 224–232. https://doi.org/10.1016/j.ijheatfluidflow.2016.10.007

Lee, P. S., Garimella, S. V., & Liu, D. (2005). Investigation of heat transfer in rectangular microchannels. *International Journal of Heat and Mass Transfer*, *48*(9), 1688–1704. https://doi.org/10.1016/j.ijheatmasstransfer.2004.11.019

Li, Z., Tao, W. Q., & He, Y. L. (2006). A numerical study of laminar convective heat transfer in microchannel with non-circular cross-section{star, open}{star, open}A preliminary version of this paper was presented at ICMM05. *International Journal of Thermal Sciences*, *45*(12), 1140–1148. https://doi.org/10.1016/j.ijthermalsci.2006.01.011

Liu, D., & Garimella, S. V. (2004). Investigation of liquid flow in microchannels. *Journal of Thermophysics and Heat Transfer*, *18*(1), 65–72. https://doi.org/10.2514/1.9124

Mehendale, S. S., Jacob, A. M., & Shah, R. K. (2000). Fluid Flow and Heat Transfer at Micro- and Meso-Scales With Application to Heat Exchanger Design. *Applied Mechanics Reviews*, *53*(7), 175–193. https://doi.org/10.1115/1.3097347

Morini, G. L. (2004). Laminar-to-turbulent flow transition in microchannels. *Microscale Thermophysical Engineering*, *8*(1), 15–30. https://doi.org/10.1080/10893950490272902

Pfund, D., Rector, D., Shekarriz, A., Popescu, A., & Welty, J. (2000). Pressure drop measurements in a microchannel. *AIChE Journal*, *46*(8), 1496–1507. https://doi.org/10.1002/aic.690460803

Qu, W., & Mudawar, I. (2002). Analysis of three-dimensional heat transfer in micro-channel heat sinks. *International Journal of Heat and Mass Transfer*, *45*(19), 3973–3985. https://doi.org/10.1016/S0017-9310(02)00101-1

Sahar, A. M., Özdemir, M. R., Fayyadh, E. M., Wissink, J., Mahmoud, M. M., & Karayiannis, T. G. (2015). Single phase flow pressure drop and heat transfer in rectangular metallic microchannels. *Applied Thermal Engineering*, *93*, 1324–1336. https://doi.org/10.1016/j.applthermaleng.2015.08.087

Satish G. Kandlikar. (2003). Microchannels and Minichannels. *First International Conference on Microchannels and Minichannels April 24-25, 2003, Rochester, New York, USA*, *i*(2002), 1–6. https://doi.org/10.1115/ICMM2003-1125

Wu, H. Y., & Cheng, P. (2003). Friction factors in smooth trapezoidal silicon microchannels with different aspect ratios. *International Journal of Heat and Mass Transfer*, *46*(14), 2519–2525. https://doi.org/10.1016/S0017-9310(03)00106-6

Yuan, X., Tao, Z., Li, H., & Tian, Y. (2016). Experimental investigation of surface roughness effects on flow behavior and heat transfer characteristics for circular microchannels. *Chinese Journal of Aeronautics*, *29*(6), 1575–1581.

https://doi.org/10.1016/j.cja.2016.10.006

Zhu, P.-F. H. and Z.-H. Y. and F. H. and K.-Q. (2006). Experimental investigation of water flow in smooth and rough silicon microchannels. *Journal of Micromechanics and Microengineering*, *16*(7), 1397. Retrieved from http://stacks.iop.org/0960-1317/16/i=7/a=037